How to cite: Angew. Chem. Int. Ed. 2024, e202421580
doi.org/10.1002/anie.202421580

Ion Transport Hot Paper

Transmembrane Delivery of an Aryl Azopyrazole Photo-switchable Ion Transporter Relay

*Elin Grählert and Matthew J. Langton**

Abstract: Stimuli-responsive synthetic ionophores allow for spatial and temporal control over ion transport, with promise for applications in targeted therapy. Relay transporters have emerged as a new class of ion transporters - these are anchored carriers that sit in both leaflets of the bilayer and mediate transport across the membrane by passing ions between them. The relays are themselves membrane impermeable, and so must be incorporated into the membrane during vesicle preparation. Here we show that relay transporters can be delivered to both sides of the membrane of vesicles using a synthetic flippase. By incorporating an aryl azopyrazole photo-switch into the movable arm of the relay transporters the ion transport activity can be very efficiently and reversibly switched between off and on states. This control is achieved by extension and contraction of their movable arms via photo-isomerization of the central aryl azopyrazole moiety, hence modulating the ability of the relays to pass ions across the membrane.

Ion transport across lipid bilayers is a fundamental process in nature,[1] and is mediated by membrane-spanning protein ion channels or pumps.[2] Genetic mutations may cause malfunction of these systems leading to diseases known as channelopathies, including cystic fibrosis, osteoporosis, and epilepsy.[3] The development of artificial stimuli-responsive ion transport systems may present an opportunity to develop therapeutics for channelopathies, and provide tools to engineer functional membranes in synthetic cells.[4] A variety of artificial ion channels that respond to a range of stimuli including light,[5] ligands,[6] and redox stimuli[7] have been explored. Mobile carriers have also been widely studied,[8] with stimuli-responsive examples including photo-,[9] pH-,[10] voltage-,[11] and redox-responsive[9c,12] systems. Contrasting with channels and mobile carriers, anchored carriers consist of an immobile component anchored in the membrane, connected to a mobile ion receptor which facilitates transport.[13] Examples include unimolecular ion shuttles,[14] ion fishers,[15] swings,[16] and rotors.[17]

In 2008, Smith et al. developed a bimolecular ion relay transport system, in which two carriers are anchored in opposite leaflets of the membrane by a lipid anchor, and transport is facilitated by passing ions between the two receptors.[18] We have subsequently reported a chloride selective halogen-bonding relay transporter,[19] and photo-responsive derivatives.[20] The latter incorporate a photo-switchable tetra-*o*-fluoro-azobenzene in the movable arm which can undergo *E*-*Z* photo-isomerisation upon irradiation with green and blue light. Only the extended *E* isomer state can facilitate ion transport, because the more contracted *Z* isomer is too short to reach into the membrane interior and pass an ion to a receptor in the opposite leaflet (cf. Figure 1a).[20a] However, incomplete photo-switching of the tetra-*o*-fluoro-azobenzene core results in a significant proportion (16 %) of the relays to be present as the (active) *E* isomer at the *Z*-rich photo-stationary state (PSS), causing significant background transport activity in this nominally 'off' state, and only a 3-fold difference in transport rates between the two isomers.

One limitation of relay transporters is that they must be present in both leaflets of the membrane, yet are themselves membrane impermeable by virtue of the lipid head group. This means that they cannot be delivered to a pre-formed membrane (i. e. a lipid vesicle or cell), and their use is therefore limited to applications in synthetic cell-like compartments where they can be incorporated into both sides of the membrane during vesicle / cell preparation. In nature, membrane-bound enzymes variously called "translocases", "scramblases" or "flippases" facilitate the translocation or "flip-flop" of lipids across the bilayer to establish asymmetric lipid distributions.[21] Low molecular weight artificial model compounds have been developed to mimic the function of these enzymes. For example, Smith et al. reported on a tris(2-aminoethyl)amine derivative with sulfonamide hydrogen-bond donors able to form a complex with a phosphatidylcholine lipid head group and mediate flip-flop across the lipid bilayer.[21–22]

Herein, we demonstrate that relay transporters can be delivered to the inner membrane leaflet of vesicles using an artificial flippase (Figure 1c), opening up the potential for delivery to pre-formed living or artificial cellular systems. We utilize this technique on novel second generation relay transporters. These exhibit highly efficient photo-switching by incorporation of a photo-switchable aryl azopyrazole moiety, enabling near quantitative reversible off-on switch-

[*] E. Grählert, Prof. M. J. Langton
Department of Chemistry, University of Oxford, Chemistry Research Laboratory
Mansfield Road, Oxford OX1 3TA (UK)
E-mail: matthew.langton@chem.ox.ac.uk

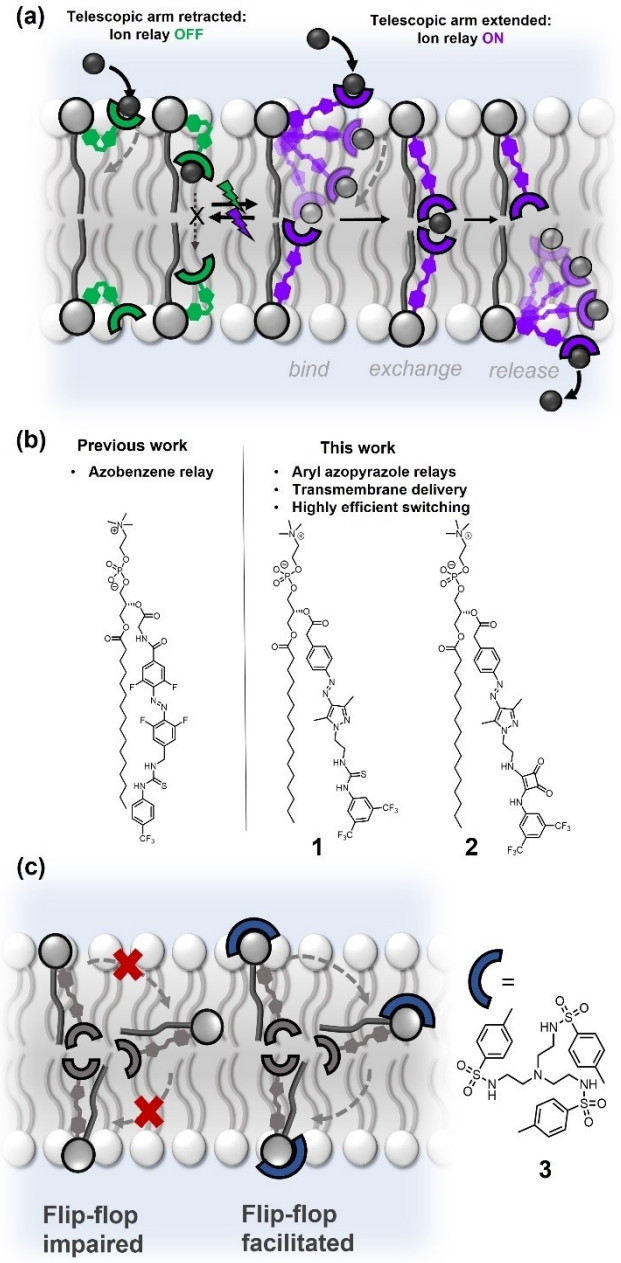

Figure 1. (a) Schematic representation of the photo-switchable relay ion transport process. (b) Structures of the previously reported azobenzene relay[20a] and the novel thiourea (**1**) and squaramide (**2**) aryl azopyrazole-based relay transporters. (c) Schematic representation of the delivery of relay transporters to the inner membrane leaflet with an artificial flippase **3**.

ing of anion transport, significantly improved over that achievable with azobenzene-derived relays. Unprecedented reversible in situ switching of relay ion transport could be achieved by alternating the irradiation wavelength of the incident light, with up to 20-fold enhancement in transport rates for the on state in comparison to the off state.

The design of the aryl azopyrazole photo-switchable relay transporters is shown in Figure 1b, and was adapted from our previously reported azobenzene-derived systems.[20] The relay is embedded into the lipid bilayer by a phosphatidylcholine lipid anchor, which is functionalized with a movable telescopic relay arm. The central feature of the arm, the photo-switchable moiety, provides a mechanism for photo-control over the ion transport. In order to address the challenge of the relatively poor on-off switching of transport activity with azobenzene derivatives, we incorporated an aryl azopyrazole molecular photo-switch. First described by Fuchter et al.,[23] these allow for near-quantitative bidirectional switching between *E*- and *Z*-isomers, with long *Z*-isomer thermal half-lives ($t_{1/2}$~10 d), and hence their incorporation into a relay was expected to improve the photo-switching of transport activity. Squaramide and thiourea anion binding sites were selected to be incorporated into the relay systems, as both motifs have been extensively utilized in a range of artificial anion transport systems,[9a,b,10a,20a,24] and previous reports suggest that squaramides facilitate higher transport rates in mobile carrier systems than their thiourea counterparts.[24a] Relay transporters **1** and **2** were prepared by coupling of a phospholysolipid with the aryl azopyrazole photo-switch, followed by installation of the thiourea or squaramide anion binding site, respectively. Full synthetic details are available in the ESI.

The ion transport activity of the relay systems was measured using an 8-hydroxypyrene-1,3,6-trisulfonic acid trisodium salt (HPTS) assay in large unilamellar vesicles (LUVs) composed of 1-palmitoyl-2-oleoyl-glycero-3-phosphocholine (POPC) in buffered NaCl solution. Transport was initiated by addition of a NaOH pulse. The ability of the relays to dissipate the pH gradient by transport of H^+ or OH^- via OH^-/Cl^- exchange (antiport) or the functionally equivalent, but osmotically disfavoured, H^+/Cl^- symport was determined by monitoring the change in the ratio of the fluorescence intensities (λ_{em} = 510 nm) of protonated (λ_{ex} = 405 nm) and deprotonated (λ_{ex} = 460 nm) HPTS with time. The ion transport activity of both relays in the *E*-rich PSS at 530 nm pre-incorporated into both membrane leaflets was studied over a range of concentrations (Figure 2a and Figure S39). The EC_{50} value (concentration required to afford half-maximal activity) for relay **1** was determined by Hill analysis to be 2.4 mol % with respect to lipid, a ~2-fold increase in activity over the previously reported azobenzene-derived relay (4.5 mol %).[20a] Squaramide relay **2** exhibited a somewhat lower activity, however, at higher loadings an instantaneous dissipation of the pH gradient was observed upon addition of the base pulse (Figure S39, 40). Given that DLS experiments indicated that the vesicle remained intact (Table S5), we suggest that the squaramide moieties, which are known to form strong intermolecular interactions,[25] stack within the lipid bilayer and lead to some membrane disruption above a critical concentration, rendering it permeable to ions. Consequently, further studies of the transport activity were focused on **1**.

The relay transport mechanism requires transporters to be present in both leaflets of the membrane (Figure 1a). When relay **1** was pre-incorporated into LUVs and thus present in both leaflets, transport activity was observed (Figure 2b). Relay **1** could alternatively be incorporated into solely the outer leaflet of the LUVs by addition of a DMSO

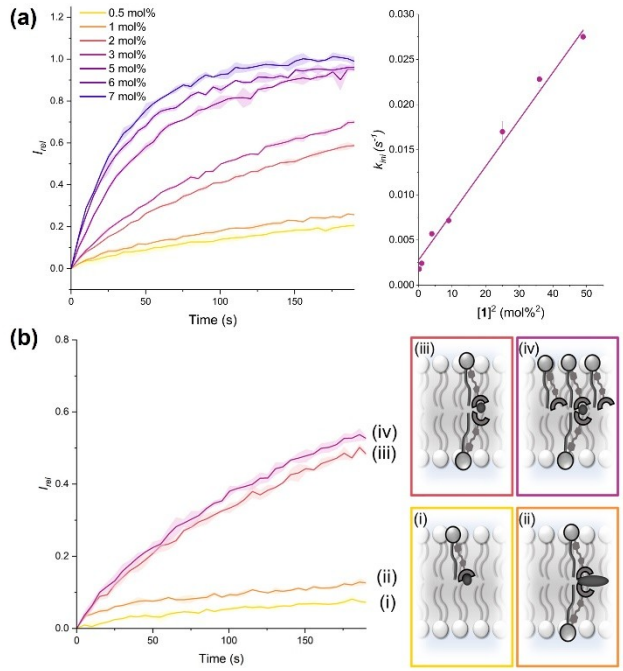

Figure 2. (*a*) Change in ratiometric emission, I_{rel} ($\lambda_{em} = 510$ nm; $\lambda_{ex1} = 405$ nm, $\lambda_{ex2} = 460$ nm), upon addition of a NaOH base pulse (5 mM) to POPC LUVs (31 μM) containing 1 mM HPTS, 100 mM internal and external NaCl, buffered with 10 mM HEPES at pH 7.0. Data for relay **1** at PSS_{530} and linear relationship of initial rate, k_{ini}, with [**1**]^2. (b) Transport activity of **1** at PSS_{530} (i) externally added (2 mol%) to LUVs; (ii) pre-incorporated (3 mol%) in NaGluconate buffer; (iii) pre-incorporated (2 mol%); (iv) with an asymmetric distribution in the outer leaflet (6 mol%) to the inner leaflet (2 mol%). Error bars and shadings represent standard deviations.

solution of **1** to pre-formed LUVs, with successful membrane uptake confirmed by UV/Vis spectroscopy (Figure S31). No ion transport was observed in this case because of the inability of the relay to cross the membrane due to the zwitterionic head group, as observed previously (Figure 2b, Figure S41).[19–20] A linear correlation between the initial rate of ion transport, k_{ini}, and the square of the transporter loading was observed (Figure 2a), indicative of two relay molecules involved in the rate determining step, supporting the proposed ion transport mechanism. Hill analysis of the fluorescence intensity at the end of the transport experiments afforded a Hill coefficient of 2, indicative of two molecules in the rate limiting step, corroborating the results of the kinetics analysis. In agreement with results reported for other relay transporters,[19–20] this implies that the rate determining step involves the breaking of the intermediate 2:1 relay:anion complex that is formed when the ion is passed from one relay to the other. This was further supported by the observation of negligible change in transport rates upon establishing an unbalanced distribution of **1** across the outer and inner membrane leaflet (3:1; outer:inner; Figure 2b, Figure S42). A lack of transport activity by **1** when the anion in the buffer was exchanged from chloride to the larger and more hydrophilic gluconate anion confirmed the transport of anions (via Cl^-/OH^- antiport or H^+/Cl^- symport) over the possible cation dependent Na^+/H^+ antiport process (Figure 2b, Figure S43).

To explore the transmembrane delivery of relay **1** to pre-formed vesicles, we prepared flippase **3**[21–22] (Figure 1c) from 4-methylbenzenesulfonyl chloride with *N1,N1*-bis(2-aminoethyl)ethane-1,2-diamine.[26] In initial experiments, relay **1** (3.5 mol% with respect to lipid) and the flippase **3** (100 mol% with respect to lipid) were mixed in DMSO to form a flippase-relay complex **1•3**, and added to LUVs. This led to activation of ion transport (Figure S44). Studying the effect of flippase concentration on relay transport activity (1.75–100 mol%) determined that optimum activity could be achieved with 14 mol% flippase (Figure 3a(i); Figure S44). In contrast, addition of only relay **1**, or flippase **3**, at the same concentrations to LUVs did not result in appreciable transport (Figure 3a(iii) and (iv)). This can be ascribed to the inability of the relay to distribute across the two leaflets of the bilayer (as discussed previously); and the poor anion transport ability of flippase **3** itself. These results demonstrate that in the presence of flippase **3**, relay **1** is delivered to both leaflets of the membrane, which is requisite to achieve relay ion transport.

To rule out a possible carrier mechanism mediated by the relay-flippase complex **1•3**, rather than the postulated relay mechanism between receptors in both leaflets, we synthesised control compound **4** (Figure 3b), which is derived from the same lyso-lipid as **1** and possesses an identical thiourea binding site, but contains an arm that is too short to allow for transport via the relay mechanism. Control compound **4** was inactive upon pre-incorporation (7 mol% loading, Figure S45) or external addition to LUVs as a DMSO solution (3.5 mol%, Figure S46; membrane-

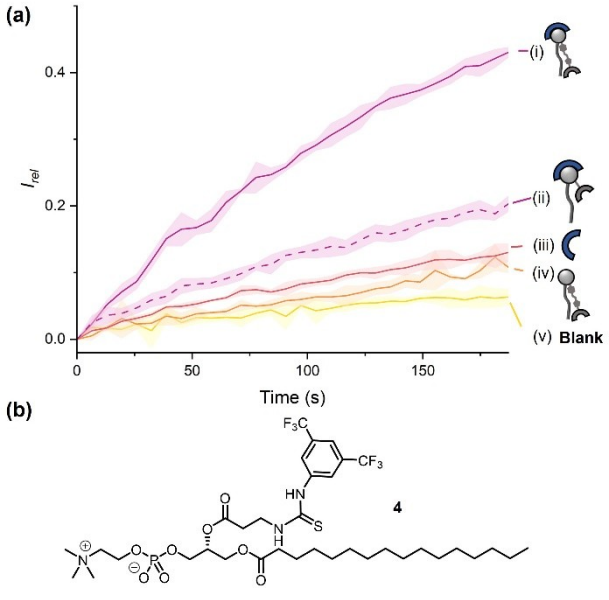

Figure 3. (a) Anion transport assays upon external additions of a mixture of (i) relay **1** (3.5 mol%) at PSS_{530} and flippase **3** (14 mol%); (ii) a mixture of **4** (3.5 mol%) and **3** (14 mol%); (iii) **1** (3.5 mol%) at PSS_{530}; (iv) **3** (14 mol%); (v) DMSO blank. (b) Structure of control compound **4**.

uptake confirmed by UV/Vis spectroscopy, Figure S32), confirming its inability to act as a relay. Addition of a mixture of **4** (3.5 mol %) and flippase (14 mol %) in DMSO to LUVs caused minimal increase of transport activity compared to the flippase (Figure 3a(ii)), demonstrating that the flippase-relay complex is unable to act as a mobile carrier, and hence that the relay mechanism with the longer derivative **1** is dominant in the anion transport process.

The photo-switching of relay **1** and **2** was studied in solution both by UV/Vis and ^{1}H NMR spectroscopy (Table 1). UV/Vis spectroscopy revealed significant red-shifting of the λ_{max} of the π–π* transition of the *E*-isomer relative to the one of the *Z*-isomer (Figure S27, S28). Thus, by excitation of the π–π* transition at 365 nm (where there is strong absorption by the *E*-isomer and minimal by the Z-isomer) the relay arm is isomerized to the Z-isomer, concomitant with a reduction in relay arm length. Exciting the tail of the n-π* band of the Z-isomer at 530 nm enables switching to the *E*-isomer and the extension of the relay arm. The PSSs at 365 and 530 nm of both relays were determined by ^{1}H NMR experiments (Figure S22, S23), revealing highly efficient bidirectional switching, much improved over that of the previously reported *tetra*-o-fluoro azobenzene relay.[20a] The PSS at 405 nm, close to the isosbestic point, was also determined. Here the *E*- and the *Z*-isomer are present in comparable amounts, a feature that we subsequently exploited for studying intermediate transport activities.

Table 1: Photo-stationary state distributions of **1**, **2** and the previously reported azobenzene relay[20a]

Relay (in solvent)	%*E* at E-rich PSS (at wavelength)	%*Z* at Z-rich PSS (at wavelength)	%*E* at isosbestic point[a]
1 (d6-DMSO)	95 (530 nm)	95 (365 nm)	40 (405 nm)
1 (2:1 $CDCl_3$/CD_3OD)	93 (530 nm)	96 (365 nm)	61 (405 nm)
1 (POPC LUVs)	96 (530 nm)	90 (365 nm)	60 (405 nm)
2 (2:1 $CDCl_3$/CD_3OD)	92 (530 nm)	90 (365 nm)	51 (405 nm)
Azobenzene relay[20a] (d6-DMSO)	95 (405 nm)	84 (530 nm)	Not reported

[a] Irradiation of **1** and **2** at 405 nm, close to the isosbestic point

Fully reversible photo-isomerisation between the *E*-rich PSS at 530 nm and the *Z*-rich PSS at 365 nm of relay **1** in LUVs was demonstrated by UV/Vis spectroscopy (Figure S33), again achieving close to quantitative photo-switching in both directions (Table 1). The ion transport activity of **1** could be successfully switched upon photo-irradiation at different wavelengths (Figure S35). The concentration dependence of the initial rates of transport of relay **1**, across the *E*-rich (530 nm), *Z*-rich (365 nm) and *E*~*Z* (405 nm) PSS distributions is shown in Figure 4a. The gradient of the linear plot of k_{ini} vs $[\mathbf{1}]^2$ represents the rate constant *k* of the transport process. The rate constant k_{530} at PSS_{530} was determined to be 20-fold greater than the rate constant k_{365} at PSS_{365}, and about double that of the rate constant k_{405} at PSS_{405}. In contrast, the previously reported azobenzene relay achieved only a 3-fold difference in the rate constants of the *E*-rich PSS compared to that of the *Z*-rich PSS (Table S4).[20a] This demonstrates that the improved photo-switching abilities of the aryl azopyrazole compared to the tetra-*o*-fluoro azobenzene directly translate to vastly improved switching of the transport activity.

Analysis of the rate constants of the three studied PSSs in conjunction with the known PSS isomer distributions allowed for further characterisation of the transport process. In principle, there are three pairwise combinations of relay isomers sitting in opposite leaflets of the bilayer that could facilitate ion transport: *EE*, *EZ* and *ZZ*. The proposed transport mechanism assumes that the contracted arms of the *Z*-isomers are too short to allow for the transfer of the ion from one arm to the other. We developed a simple kinetic model to determine of the relative activities of each pairwise interaction from this data (see ESI), which revealed that the *ZZ* combination is inactive, whereas both *EE* and *EZ* facilitate transport. The fully extended *EE* pairwise interaction is 5x more active than the mixed *EZ* interaction,

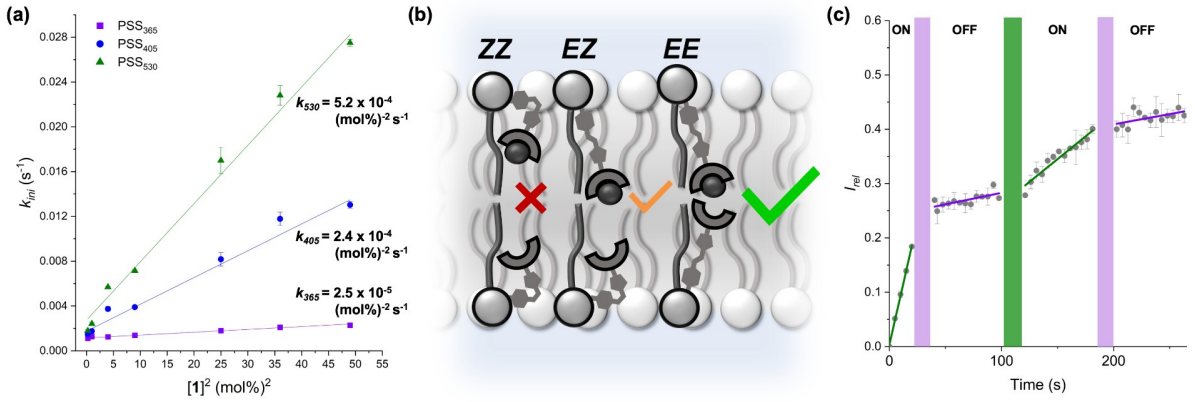

Figure 4. (a) Linear dependence of k_{ini} on $[\mathbf{1}]^2$ at PSS_{365}, PSS_{405} and PSS_{530} generated by in situ isomerisation and corresponding rate constants. (b) Schematic representation of inactive and active relay isomer combinations for ion transport (c) In situ, real-time switching of ion transport mediated by **1** (3 mol %) pre-irradiated at 530 nm, with subsequent irradiation at 365 nm (purple) and 530 nm (green) light from an LED for 10 s.

in agreement with the proposed mechanism (Figure 4b, Table S3).

Finally, we exploited the efficient and reversible switching capability of **1** for unprecedented real-time, in situ control over relay ion transport by irradiating the relays within the membrane of LUVs. On to off switching of LUVs pre-irradiated with 530 nm light could be achieved at various time points during a transport experiment by 10 s of irradiation with 365 nm light (Figure S47). Repetitive on→off→on→off switching of activity could also be achieved by successive irradiation at 365 nm and 530 nm for 10 s, (Figure 4c), to facilitate temporal control over relay activity.

In conclusion, by using a synthetic flippase we demonstrated delivery of relay transporters to the inner leaflet of the lipid bilayer. By utilizing an aryl azopyrazole photoswitch, we were able to develop relays with significantly enhanced photo-switching properties compared to previously developed azobenzene derivatives. The improved PSSs directly translate into greatly enhanced photo-switching of the transport activity, allowing for real-time on and off switching of anion transport. Kinetics analysis revealed that the on state is 20-times more active than the off state, and confirmed that *E-E* pairwise interactions dominate the relay mechanism. We anticipate that the ability to both carefully control the transport activity of relays using light in a reversible manner, coupled with the capacity to deliver these species across membranes using synthetic flippases, may open up new avenues for the application of relay transporters in both synthetic and living cells.

Supporting Information

The authors have cited additional references within the Supporting Information[20a,26–27]

Acknowledgements

E. G. thanks the EPSRC Centre for Doctoral Training in Inorganic Chemistry for Future Manufacturing (OxICFM, EP/S023828/1) for studentship funding. We thank Dr Aidan Kerckhoffs and Dr Toby Johnson for useful discussion, and Anna Duncan and Prof. Jason Davis, University of Oxford, for assistance with and access to DLS. M. J. L. is a Royal Society University Research Fellow.

Conflict of Interest

The authors declare no conflict of interest.

Data Availability Statement

The data that support the findings of this study are available in the supplementary material of this article.

Keywords: Ionophores · lipids membranes · phospholipids · photo-switch · vesicles

[1] J. T. Davis, O. Okunola, R. Quesada, *Chem. Soc. Rev.* **2010**, *39*, 3843–3862.
[2] D. L. Neverisky, G. W. Abbott, *Crit. Rev. Biochem. Mol. Biol.* **2016**, *51*, 257–267.
[3] F. M. Ashcroft, *Nature* **2006**, *440*, 440–447.
[4] M. J. Langton, *Nat. Chem. Rev.* **2021**, *5*, 46–61.
[5] a) Y. Zhou, Y. Chen, P.-P. Zhu, W. Si, J.-L. Hou, Y. Liu, *Chem. Commun.* **2017**, *53*, 3681–3684; b) T. Liu, C. Bao, H. Wang, Y. Lin, H. Jia, L. Zhu, *Chem. Commun.* **2013**, *49*, 10311–10313; c) P. V. Jog, M. S. Gin, *Org. Lett.* **2008**, *10*, 3693–3696.
[6] a) Q. Xiao, W.-W. Haoyang, T. Lin, Z.-T. Li, D.-W. Zhang, J.-L. Hou, *Chem. Commun.* **2021**, *57*, 863–866; b) T. Muraoka, D. Noguchi, R. S. Kasai, K. Sato, R. Sasaki, K. V. Tabata, T. Ekimoto, M. Ikeguchi, K. Kamagata, N. Hoshino, H. Noji, T. Akutagawa, K. Ichimura, K. Kinbara, *Nat. Commun.* **2020**, *11*, 2924.
[7] a) J. A. Malla, R. M. Umesh, S. Yousf, S. Mane, S. Sharma, M. Lahiri, P. Talukdar, *Angew. Chem. Int. Ed.* **2020**, *59*, 7944–7952; b) L. Shi, W. Zhao, Z. Jiu, J. Guo, Q. Zhu, Y. Sun, B. Zhu, J. Chang, P. Xin, *Angew. Chem. Int. Ed.* **2024**, *63*, e202403667.
[8] a) P. A. Gale, J. T. Davis, R. Quesada, *Chem. Soc. Rev.* **2017**, *46*, 2497–2519; b) J. T. Davis, P. A. Gale, R. Quesada, *Chem. Soc. Rev.* **2020**, *49*, 6056–6086; c) A. P. Davis, D. N. Sheppard, B. D. Smith, *Chem. Soc. Rev.* **2007**, *36*, 348–357.
[9] a) S. J. Wezenberg, L.-J. Chen, J. E. Bos, B. L. Feringa, E. N. W. Howe, X. Wu, M. A. Siegler, P. A. Gale, *J. Am. Chem. Soc.* **2022**, *144*, 331–338; b) A. Kerckhoffs, M. J. Langton, *Chem. Sci.* **2020**, *11*, 6325–6331; c) M. Ahmad, T. G. Johnson, M. Flerin, F. Duarte, M. J. Langton, *Angew. Chem. Int. Ed.* **2024**, *63*, e202403314; d) Y. R. Choi, G. C. Kim, H.-G. Jeon, J. Park, W. Namkung, K.-S. Jeong, *Chem. Commun.* **2014**, *50*, 15305–15308; e) M. Ahmad, S. Metya, A. Das, P. Talukdar, *Chem. Eur. J.* **2020**, *26*, 8703–8708; f) S. B. Salunke, J. A. Malla, P. Talukdar, *Angew. Chem. Int. Ed.* **2019**, *58*, 5354–5358.
[10] a) L. A. Marchetti, T. Krämer, R. B. P. Elmes, *Org. Biomol. Chem.* **2022**, *20*, 7056–7066; b) S. Rashdan, M. E. Light, J. D. Kilburn, *Chem. Commun.* **2006**, 4578–4580; c) N. Busschaert, R. B. P. Elmes, D. D. Czech, X. Wu, I. L. Kirby, E. M. Peck, K. D. Hendzel, S. K. Shaw, B. Chan, B. D. Smith, K. A. Jolliffe, P. A. Gale, *Chem. Sci.* **2014**, *5*, 3617–3626.
[11] X. Wu, J. R. Small, A. Cataldo, A. M. Withecombe, P. Turner, P. A. Gale, *Angew. Chem. Int. Ed.* **2019**, *58*, 15142–15147.
[12] a) A. Docker, T. G. Johnson, H. Kuhn, Z. Zhang, M. J. Langton, *J. Am. Chem. Soc.* **2023**, *145*, 2661–2668; b) N. Akhtar, O. Biswas, D. Manna, *Org. Biomol. Chem.* **2021**, *19*, 7446–7459; c) M. Fares, X. Wu, D. Ramesh, W. Lewis, P. A. Keller, E. N. W. Howe, R. Pérez-Tomás, P. A. Gale, *Angew. Chem. Int. Ed.* **2020**, *59*, 17614–17621; d) G. Park, F. P. Gabbaï, *Chem. Sci.* **2020**, *11*, 10107–10112; e) S. Das, O. Biswas, N. Akhtar, A. Patel, D. Manna, *Org. Biomol. Chem.* **2020**, *18*, 9246–9252.
[13] a) T. G. Johnson, M. J. Langton, *J. Am. Chem. Soc.* **2023**, *145*, 27167–27184; b) J. Shen, C. Ren, H. Zeng, *Acc. Chem. Res.* **2022**, *55*, 1148–1159.
[14] a) S. Chen, Y. Wang, T. Nie, C. Bao, C. Wang, T. Xu, Q. Lin, D.-H. Qu, X. Gong, Y. Yang, L. Zhu, H. Tian, *J. Am. Chem. Soc.* **2018**, *140*, 17992–17998; b) C. Wang, S. Wang, H. Yang, Y. Xiang, X. Wang, C. Bao, L. Zhu, H. Tian, D.-H. Qu, *Angew. Chem. Int. Ed.* **2021**, *60*, 14836–14840.

[15] R. Ye, C. Ren, J. Shen, N. Li, F. Chen, A. Roy, H. Zeng, *J. Am. Chem. Soc.* **2019**, *141*, 9788–9792.
[16] C. Ren, F. Chen, R. Ye, Y. S. Ong, H. Lu, S. S. Lee, J. Y. Ying, H. Zeng, *Angew. Chem. Int. Ed.* **2019**, *58*, 8034–8038.
[17] H. Yang, J. Yi, S. Pang, K. Ye, Z. Ye, Q. Duan, Z. Yan, C. Lian, Y. Yang, L. Zhu, D.-H. Qu, C. Bao, *Angew. Chem. Int. Ed.* **2022**, *61*, e202204605.
[18] B. A. McNally, E. J. O'Neil, A. Nguyen, B. D. Smith, *J. Am. Chem. Soc.* **2008**, *130*, 17274–17275.
[19] T. G. Johnson, A. Docker, A. Sadeghi-Kelishadi, M. J. Langton, *Chem. Sci.* **2023**, *14*, 5006–5013.
[20] a) T. G. Johnson, A. Sadeghi-Kelishadi, M. J. Langton, *J. Am. Chem. Soc.* **2022**, *144*, 10455–10461; b) T. G. Johnson, A. Sadeghi-Kelishadi, M. J. Langton, *Chem. Commun.* **2024**, *60*, 7160–7163.
[21] J. M. Boon, B. D. Smith, *J. Am. Chem. Soc.* **1999**, *121*, 11924–11925.
[22] a) J. M. Boon, B. D. Smith, *J. Am. Chem. Soc.* **2001**, *123*, 6221–6226; b) J. M. Boon, T. N. Lambert, B. D. Smith, A. M. Beatty, V. Ugrinova, S. N. Brown, *J. Org. Chem.* **2002**, *67*, 2168–2174.
[23] C. E. Weston, R. D. Richardson, P. R. Haycock, A. J. P. White, M. J. Fuchter, *J. Am. Chem. Soc.* **2014**, *136*, 11878–11881.
[24] a) N. Busschaert, I. L. Kirby, S. Young, S. J. Coles, P. N. Horton, M. E. Light, P. A. Gale, *Angew. Chem. Int. Ed.* **2012**, *51*, 4426–4430; b) L. E. Bickerton, M. J. Langton, *Chem. Sci.* **2022**, *13*, 9531–9536; c) D. A. McNaughton, E. York, T. Rawling, P. A. Gale, *Org. Biomol. Chem.* **2024**, *22*, 4868–4876; d) X. Wu, P. A. Gale, *J. Am. Chem. Soc.* **2016**, *138*, 16508–16514; e) N. Busschaert, S.-H. Park, K.-H. Baek, Y. P. Choi, J. Park, E. N. W. Howe, J. R. Hiscock, L. E. Karagiannidis, I. Marques, V. Félix, W. Namkung, J. L. Sessler, P. A. Gale, I. Shin, *Nat. Chem.* **2017**, *9*, 667–675.
[25] a) S. Bujosa, E. Castellanos, A. Frontera, C. Rotger, A. Costa, B. Soberats, *Org. Biomol. Chem.* **2020**, *18*, 888–894; b) S. Sen, A. Basu, T. Sen, G. N. Patwari, *J. Phys. Chem. A* **2020**, *124*, 5832–5839; c) A. Portell, R. Barbas, D. Braga, M. Polito, C. Puigjaner, R. Prohens, *CrystEngComm* **2009**, *11*, 52–54.
[26] C. M. Wallen, J. Bacsa, C. C. Scarborough, *J. Am. Chem. Soc.* **2015**, *137*, 14606–14609.
[27] a) A. J. Boddy, D. P. Affron, C. J. Cordier, E. L. Rivers, A. C. Spivey, J. A. Bull, *Angew. Chem. Int. Ed.* **2019**, *58*, 1458–1462; b) X. Wang, A. Kerckhoffs, J. Riexinger, M. Cornall, M. J. Langton, H. Bayley, Y. Qing, *BioRxiv.* **2024**, DOI:10.1101/2024.11.23.624940 ; c) T. Kasagami, I.-H. Kim, H.-J. Tsai, K. Nishi, B. D. Hammock, C. Morisseau, *Bioorg. Med. Chem. Lett.* **2009**, *19*, 1784–1789; d) R. M. Bennett, W. Sun, D. C. Wilson, M. E. Light, D. C. Harrowven, *Chem. Commun.* **2021**, *57*, 5694–5697; e) E. Fasoli, A. Arnone, A. Caligiuri, P. D′Arrigo, L. de Ferra, S. Servi, *Org. Biomol. Chem.* **2006**, *4*, 2974–2978; f) J. S. Stover, J. Shi, W. Jin, P. K. Vogt, D. L. Boger, *J. Am. Chem. Soc.* **2009**, *131*, 3342–3348.

Manuscript received: November 6, 2024
Accepted manuscript online: November 26, 2024
Version of record online: ■■, ■■

Communication

Ion Transport

E. Grählert, M. J. Langton* _ **e202421580**

Transmembrane Delivery of an Aryl Azopyrazole Photo-switchable Ion Transporter Relay

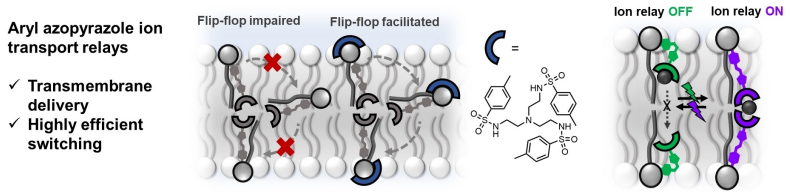

The delivery of anion relay transporters across lipid membranes using a synthetic flippase is reported. These second generation photo-responsive relays incorporate an aryl azopyrazole photo-switch enabling greatly improved reversible photo-switching of the ion transport activity in situ, in real time.